

ANALYSIS OF SURFACE CONCENTRATION OF BLACK CARBON IN RIAU PROVINCE DURING THE 2019 FOREST FIRES USING MERRA-2 REANALYSIS DATA

Wilin Julian Sari^{1*}, Dita Fatria Andarini¹, Fildzah 'Adany¹, Waluyo Eko Cahyono¹

¹Indonesia National Research and Innovation Agency (BRIN), Jalan Djunjunan 133, Bandung, 40173

*E-mail wilin.julian.sari@brin.go.id

Naskah masuk: 21 Agustus 2021 Naskah diperbaiki: 11 Februari 2022 Naskah diterima: 11 Februari 2022

ABSTRACT

Indonesia experienced forest fires almost every year, especially in the area of Riau Province, where as a result, pollutants such as carbon dioxide and black carbon are present in the air over Riau. Due to its size and its light absorption ability, black carbon is known to have bad impacts on the climate. This study aims to analyse the effect of forest fires that happened in Riau Province, Indonesia in September 2019 towards the production of black carbon, as well as to estimate backward air movement trajectory in order to confirm the air mass sources of the black carbon. The data of black carbon concentration used in this study is an hourly temporal data of MERRA-2 with a spatial resolution of $0.5^\circ \times 0.625^\circ$, while the trajectory calculation uses the HYSPLIT trajectory model. Linear regression of this study has an r -value of 0.78 which shows that there is a positive correlation between black carbon concentration and the number of hotspots. The range of BC concentrations was $2-11 \times 10^{-9} \text{ kg.m}^{-3}$ with higher concentration occurred during 9–23 September 2019 where it was affected by the south-easterly wind from Jambi and South Sumatera.

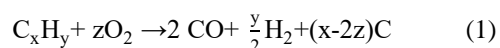
Keywords: forest fire, black carbon, MERRA-2, HYSPLIT.

1. Introduction

Tropical forests in Indonesia are the third-largest in the world with an area of 94.1 million hectares (ha) as of 2019 [1]. However, it is decreasing every year due to forest fires. According to Indonesian National Board for Disaster Management (BNPB) data, the average burned area due to forest fires is 757,787.31 ha/year (2014–2018). BNPB classified Indonesia into four areas based on the risk of experiencing forest fires, namely very high, high, medium, and low-risk areas, where Riau Province is categorized as a very high risk area [2]. Forest fires in Riau have been recorded since 1982, typically taking place every dry season, and the largest forest fires occurred in 1997–1998 due to the El Nino event [3]. In 2019, El Nino came across Indonesia and forest fire incidents were reported in Riau. There were 1347 hotspots, observed by the Aqua-Modis satellite, and 90,550 ha were burned.

Forest fire is a process of biomass combustion that emits pollutants, such as carbon dioxide (CO_2), carbon monoxide (CO), methane (CH_4), nitrogen oxides (NO_x), ammonia, volatile organic compounds (VOCs), carbonyl sulfide, sulfur dioxide, and particulate matters. These pollutants will affect the composition of the atmosphere, the carbon cycle, air quality, environmental acidity, and human health [4]. In addition, particulate matters released during forest

fires can transport thousands of kilometers to other regions [5]. Particulate matters consist of several compounds, one of which is black carbon, which is produced from the incomplete combustion of fuel or biomass, following the reaction equation below (C_xH_y is fuel or biomass and C is black carbon) [6]:



Black carbon has an effect on global warming owing to the fact that it can warm the atmosphere by absorbing solar radiation. This condition causes the absorbed light radiation on the Earth's surface to decrease, hence affecting the net-effect system on Earth-atmosphere (radiative forcing), and as a result, increasing the temperature at the surface (by $0.5-1.0^\circ\text{C}$) and the atmosphere [7]. Furthermore, black carbon deposited on snow can reduce the snow's albedo so that it melts faster [6]. The lifetime of black carbon is short (7–10 days), but its global warming potential (GWP) is 5000 times higher than CO_2 [8]. Moreover, Radiative Forcing (RF) of black carbon is $1-1.2 \text{ Wm}^{-2}$ ($\pm 0.4 \text{ Wm}^{-2}$), second to CO_2 . Unfortunately, although black carbon is a primary pollutant from a forest fire and has an impact on global warming, there are still very few studies about black carbon in Indonesia, particularly in Riau. Therefore, this study investigates black carbon concentration produced during the dry season of 2019 forest fire

event in Riau Province and its relation to hotspots using Modern-Era Retrospective analysis for Research and Applications, version 2 (MERRA-2) reanalysis data.

2. Methods

Data. The hourly black carbon (BC) data from MERRA-2 with a spatial resolution of $0.5^\circ \times 0.625^\circ$, accessible through the website of Giovanni (<https://giovanni.gsfc.nasa.gov/giovanni>), was used in this study. MERRA-2 reanalysis is the newest reanalysis method developed by the National Aeronautics and Space Administration (NASA) where it is an emphasized assimilation from multiple satellites since 1980. Additionally, MERRA-2 was simulated using the latest version of the Goddard Earth Observing System Model version 5 (GEOS-5) system assimilation data [9].

In order to identify the number of hotspots, we utilized the Aqua-Modis satellite with a spatial resolution of 1000m [10] obtained from <http://modis-catalog.lapan.go.id/monitoring>. Hotspots are determined by the thermal activity layer in Modis instrument and corrected by de-stripping and geometric correction process. As a consequence, Modis employs a detection algorithm to determine fire pixels that represent active burning fires when the satellite passes through a location. The bands used for this detection algorithm are band 1 (0.65 μm), band 2 (0.86 μm), band 7 (21 μm), band 21 (4 μm), band 22 (4 μm), band 31 (11 μm), and band 32 (12 μm) [11]. Further, Modis' detection algorithm goes through seven steps of identification when determining the hotspots [12], namely:

1. Land and water masking,
2. Cloud masking,
3. Identification of potential fire pixels,
4. Background characterization,
5. Tentative fire detection,
6. Rejection test, and
7. Fire detection confidence.

Afterwards, the resulted hotspots are classified into three level of confidence, as shown in table 1.

Table 1. Hotspot's Level of Confidence

Confidence Level	Classification
0%-30%	Low
30%-80%	Medium
80%-100%	High

This hotspot's confidence level shows the quality of fire pixels where the worst imagery of fire pixels will fall into the category of low confidence level. A high confidence level offers maximum fire detectability, therefore we only selected the hotspots with a high level of confidence ($> 80\%$) for this study.

In addition, the 4-times daily data of wind components from ECMWF Reanalysis v5 (ERA-5) were used to analyse the vertical structure of wind during the forest fire event. ERA-5 is the fifth generation of atmospheric reanalysis data produced by the European Centre for Medium-Range Weather Forecasts (ECMWF) that replaces ERA-Interim since 31 August 2019 [13]. ERA-5 reanalysis data has a horizontal resolution of 31 km (0.28125 degrees) and 137 vertical levels to 1 Pa [14].

Methods. Analysis of interannual variation of BC and hotspot in this study focuses on the Asian Summer Monsoon during June–July–August–September (JJAS) between 2014 and 2020. Then, spatiotemporal variations of BC concentration were calculated by composite averaged MERRA-2 reanalysis data over Riau Province (1.083°S – 2.42°N , 100°E – 104°E) in those periods. Moreover, a linear regression method is applied to determine the relationship between hotspots and BC surface concentration. The strength of this relationship is measured by a correlation coefficient (r) with a value between 0 and 1. In detail, the value of $r=1$ indicates a strong correlation, while $r=0$ means the variables do not correlate [15].

To analyse the spatiotemporal variation of BC associated with hotspots during the forest fire event in September 2019, we conducted a composite analysis by dividing the data into five periods that represent an early stage of forest fire, during the peak of the forest fire, and the end period of the forest fire. Afterwards, backward trajectories of the three days of highest BC concentrations were estimated using HYbrid Single-Particle Lagrangian Integrated Trajectory (HYSPLIT) model [14] to confirm the BC content source in Riau. We selected the Global Forecast System (GFS) data with a spatial resolution of $0.25^\circ \times 0.25^\circ$ as meteorological input and 500m Above Ground Level (AGL) for the height of the source in the model input [17].

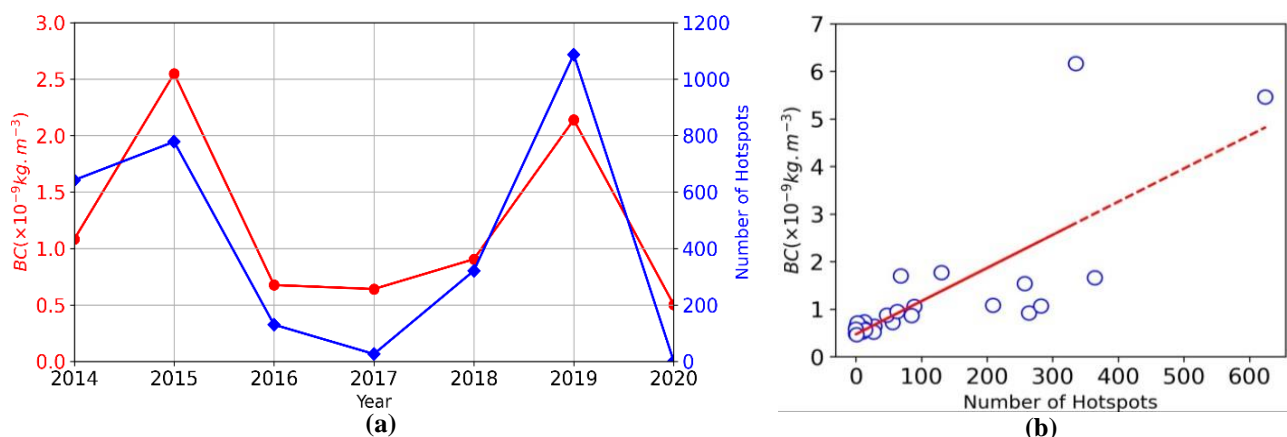


Figure 1. BC surface concentration in Riau Province (1.083°S–2.42°N, 100°E–104°E) in June–September over six years (from 2014 to 2020) (red line) (a) and the number of hotspots (blue line) Linear regression of BC surface concentration in Riau Province and the number of hotspots (b).

3. Result and Discussion

Interannual variations of BC over Riau Province.

In Figure 1a, the red line represents BC surface concentration in June–September over six years (from 2014 to 2020) in Riau Province (1.083°S–2.42°N, 100°E–104°E) and the blue line shows the number of hotspots. A previous study by Arisman about forest fire incidents trend in Indonesia suggested that there are three conditions that can trigger a forest fire, namely biomass, oxygen and/or fire source, and dryness (e.g. summer season) [18]. The dry season in Indonesia normally occurs in JJAS which is associated with Asian Summer Monsoon [19]. Asian summer Monsoon happens when the northern hemisphere has low pressure, thus, the dry air flows from the southern to northern hemisphere across the equator.

During those periods, many regions in Indonesia receive less amount of rainfall [20] wherein this condition threatens to increase forest fire incidents [21, 22]. Figure 1a suggests that during those six years, maximum concentrations of BC happened in 2015 and 2019 and minimum concentrations of BC in 2016 and 2017. These are in agreement with the number of hotspots that have maximums in 2015 and 2019 and minimums in 2016 and 2017. The dry season of 2015 and 2019 are identified as abnormally dry years since they are accompanied by El Nino events [23, 24]. Many previous studies revealed that El Nino events tend to decrease rainfall over Indonesia Maritime Continent (IMC) [25], hence prolonging the dry season which then leads to severe forest fires.

A similar relation pattern of BC and number of hotspots is demonstrated by a linear regression calculation, displayed in figure 1b, with correlation coefficient (r) 0.78 ($r^2=0.6081$). From the r -value of this linear regression, it can be deduced that BC surface concentration corresponds well with the

number of hotspots [15] in which the more the hotspot is, the higher the BC surface concentration will be. This deduction coincides with Sitnov *et al.* (2019) study where their linear regression model, $r=0.73$, denoted that BC content is directly proportional to active fires in Northern Eurasia [26].

Case study of 2019 forest fire. According to a 2019 report from the Indonesian Ministry of Environment and Forestry [27], 2019 is one of the biggest forest fires that happened in recent years where 90,550 ha of forest and land in Riau were burned. And as illustrated in figure 1a, 2019 is the second-highest in both BC mean surface concentration and the number of hotspots, as well as the most current event compared to the other years in the aforementioned period, hence we decided to focus our study on the forest fires of that year. Figure 2 portrays that BC concentration (red line) in Riau only experienced a surge during the forest fire event in September, marked by the number of hotspots (blue line). In detail, the BC surface concentration reached a peak of approximately $5.5 \times 10^{-9} \text{ kg} \cdot \text{m}^{-3}$, while just above 600 hotspots are detected by satellite in the same period. This finding is in line with the forest fire trend in Indonesia wherein the peak of hotspot distributions in 2016–2019 always occurred in September [18].

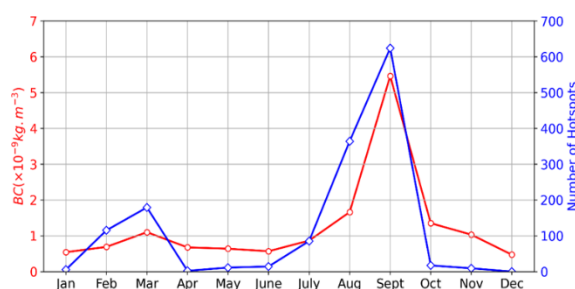


Figure 2. BC surface concentration and number of hotspots in Riau Province in 2019.

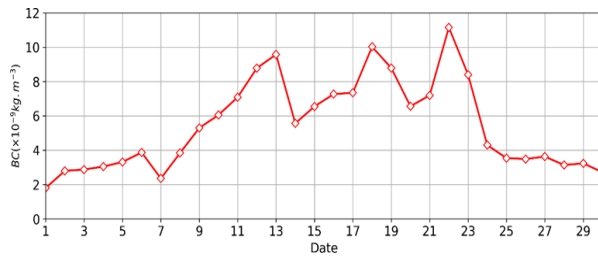


Figure 3. Daily BC surface concentration over Riau Province (1.083°S–2.42°N,100°E–104°E) in September 2019.

In order to see the progress of BC concentration on its peak month, a daily time series of BC concentration during September 2019 is presented in figure 3. As can be seen in figure 3, the range of BC concentrations was $2\text{--}11 \times 10^{-9} \text{ kg.m}^{-3}$ with higher concentration transpired during 9–23 September and three peaks took place on 13, 18, and 22 September. Moreover, in figure 4, a spatiotemporal variation analysis was carried out to wholly investigate the distributions of BC concentration and number of hotspots. The spatiotemporal variation analysis gives us information that in the first period (a) when the number of hotspots was small, the concentration of

BC was still low. Then, as the number of hotspots progressed in the second period (b), the concentration of BC was also increasing although it was not significant as of yet. Subsequently, immediately upon a step-up of the number of hotspots during the third and fourth period (c and d), the concentration of BC on those two periods was also escalated, especially in the southern part of Riau, with a local-maxima on 22 September. And finally, with a big drop in the number of hotspots in the fifth period (e), the concentration of BC was decreasing.

As shown in the spatial distributions in figure 4 (a-e), the concentration of BC in the southern part of Riau was higher than that of in the northern part. Intergovernmental Panel on Climate Change (IPCC) reported that BC has an atmospheric lifetime of 7–10 days and since BC originated from biomass combustion has an average size of $0.065\text{--}0.15 \mu\text{m}$ [9], this type of BC is able to experience a long-range transport [28]. It is predicted that the higher concentration of BC in the southern part of Riau ensued from BC particles of southern parts of Sumatra's forest fires that traveled to Riau, such as Jambi.

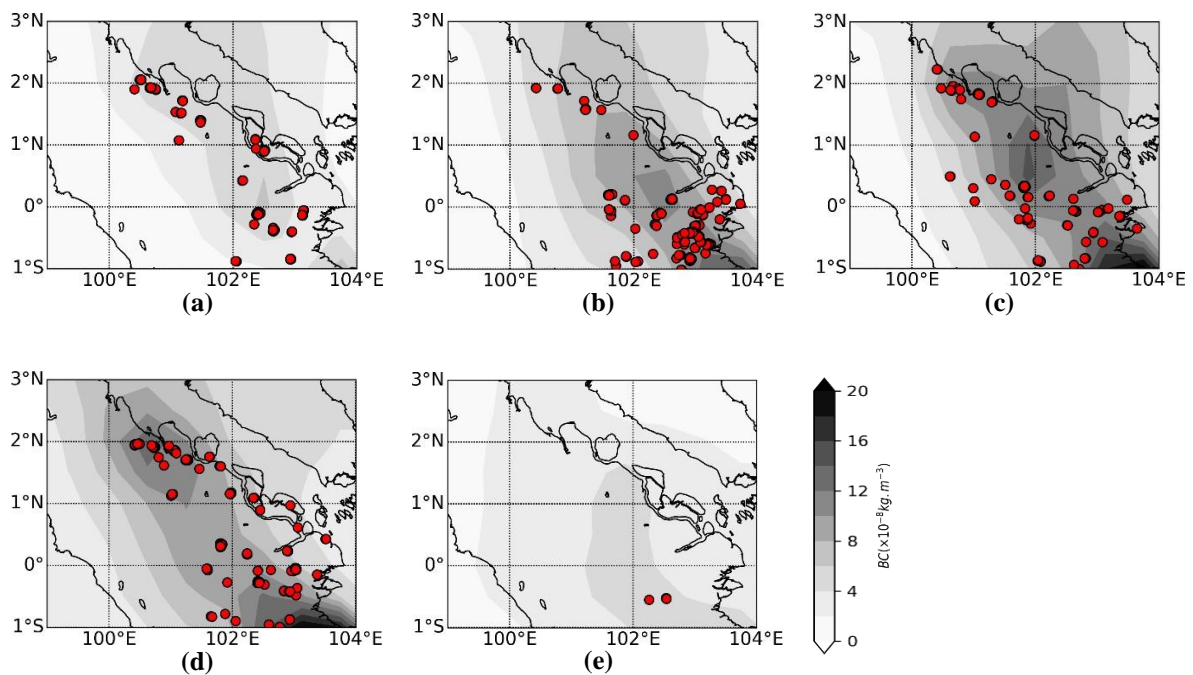


Figure 4. Spatiotemporal variation of BC mean surface concentration according to MERRA-2 reanalysis data (shading) and number of hotspots according to AQUA (red symbols) over Riau Province in September 2019: (a) 1–6 September 2019, (b) 7–12 September 2019, (c) 13–18 September 2019, (d) 19–24 September 2019, (e) 25–30 September 2019.

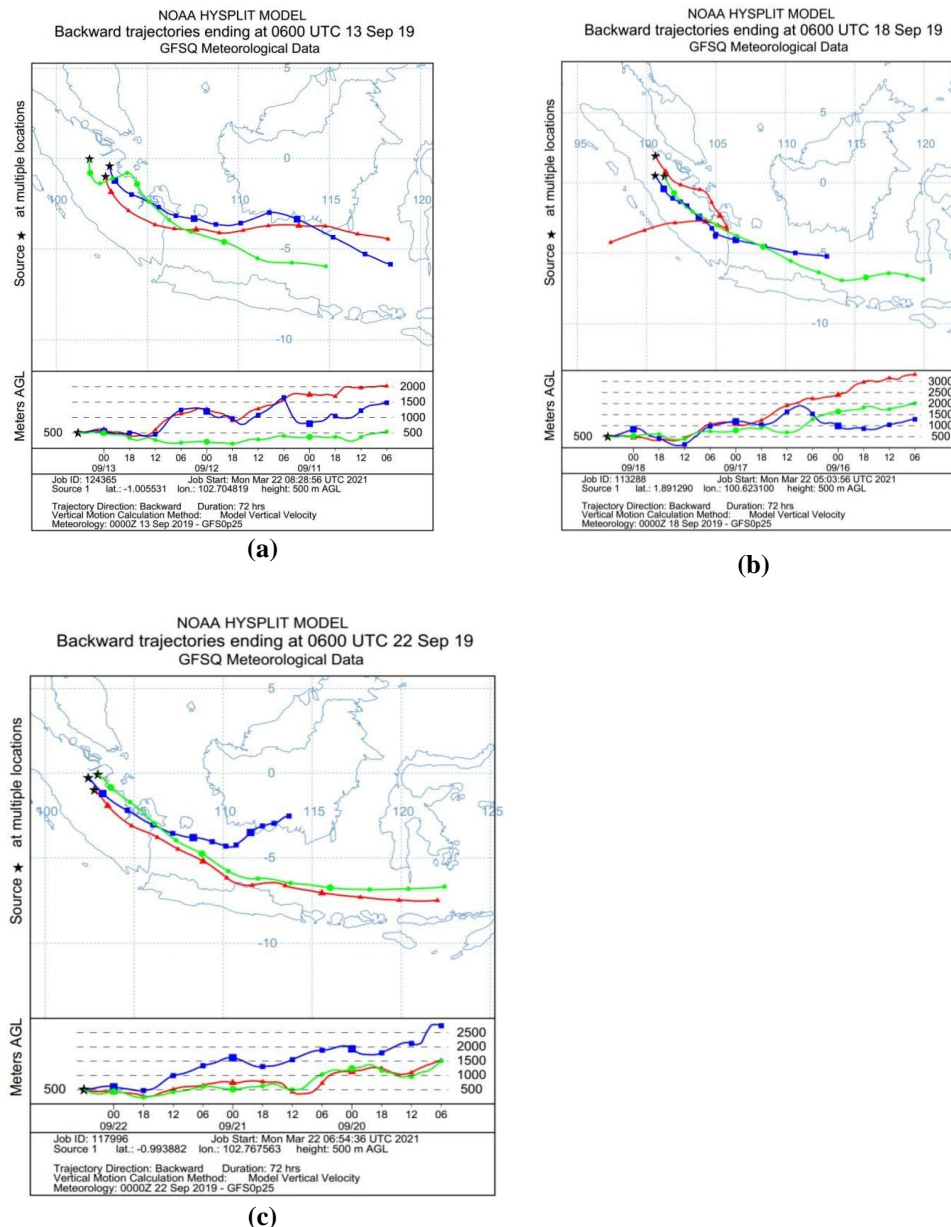


Figure 5. Backward HYSPLIT trajectories of Riau on (a) 13 September 2019, (b) 18 September 2019, (c) 22 September 2019.

To ensure whether BC in Riau was sourced from Riau Province only or whether it was affected by the neighboring provinces, trajectory estimations for the three days of BC's highest surface concentration, namely 13, 18, and 22 September 2019, were run using HYSPLIT. Figure 5 (a–c) shows that the BC concentration in 500 meters above ground level (AGL) came from several regions in the southern part of Riau, such as Jambi and South Sumatra. The backward trajectories suggested that the south-easterly wind brings the BC particles from Jambi and South Sumatra a few days earlier. This trajectory pattern dominantly occurred in the surface to around 2.5 km AGL. This situation is associated with the Asian Summer Monsoon which has a pronounced feature as easterly winds along the equator in around

850 hPa [29].

Interestingly, all trajectories passed through Jambi one day before they arrived in Riau at varying altitudes. And as it has been known, similar to Riau, Jambi experienced terrifying forest fires in 2019, particularly in September, where 56,593 ha of land and forest were burned [27] and the sky in Jambi turned to blackish-red due to the immense presence of BC. Therefore, the increase in BC surface concentration over Riau province was affected by BC particles travelling from other forest fire areas next to its south, especially Jambi.

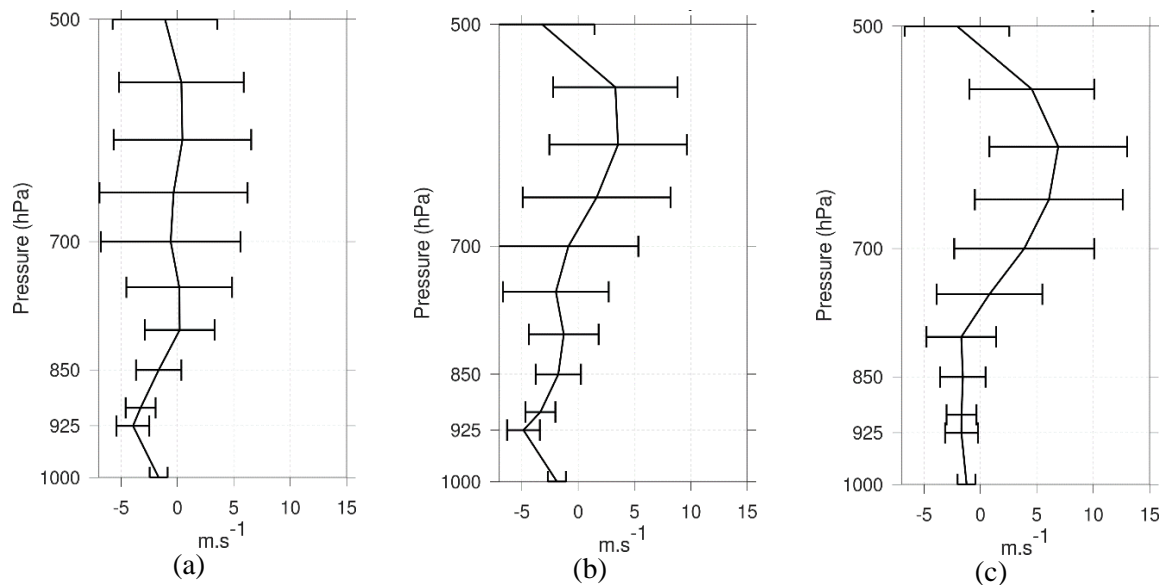


Figure 6. Zonal wind profiles averaged along 2°S–1°S, 102°E–104°E on (a) 12 September 2019, (b) 17 September 2019, and (c) 21 September 2019.

In 2019, Sitnov *et al.* used zonal wind profiles to strengthen their explanation about long-range transfer of air masses in their study. Hence, in this study, we also employed zonal wind profiles to corroborate the result of our backward HYSPLIT trajectories. The zonal wind profiles over Jambi Province (2°S–1°S, 102°E–104°E) one day before the BC concentration in Riau reached its peaks during September 2019 (12, 17, and 21 September 2019) were plotted to confirm the trajectory of BC in Riau as shown in figure 6. It can be seen that the easterly wind dominated the lower troposphere (from 1000 hPa to 800 hPa) in those days with the highest wind speed occurred at around 950 hPa or ≈ 0.5 –1 km above mean sea level. This condition favoured the transport of BC particles over Jambi to Riau as shown in figure 5 which mostly happened at about 0.5–2.5 km AGL. On the contrary, the zonal wind profiles above 700 hPa were identified as the westerly wind which has higher variation to its zonal wind mean during September 2019. Thus, it also can influence the BC transfer at a higher altitude.

4. Conclusion

Using hourly time series data from MERRA-2, BC surface concentration in the event of 2019 forest fires in Riau was successfully illustrated. It is revealed that the concentration of BC will increase when there is a forest fire event. Moreover, as suggested by the linear regression calculation, the concentration of BC has a positive correlation towards the number of hotspots with the correlation coefficient (r) 0.78, where the more the hotspot is, the higher the concentration of BC will be. During this event, the range of BC concentrations was 2 – 11×10^{-9} kg.m⁻³ with higher concentrations occurred from 9 to 23 September. According to its spatial distributions, the concentrations of BC in the southern part of Riau

were higher than that of the northern part. In addition, since BC particles are capable of experiencing long-range transport, the BC content in Riau Province was affected by BC particles from its southern neighbouring provinces, such as Jambi. This condition is confirmed by the backward trajectory of HYSPLIT analysis and zonal wind profiles over Jambi.

Acknowledgement

This work is a part of National Priority Research with the grant number No.253/E1/PRN/2020 carried out in Center of Atmospheric Science and Technology (PSTA) – Indonesia National Institute of Aeronautics and Space (LAPAN). And we are thankful for all people who supported us in writing this paper.

References

- [1] Sagala S, Sitinjak E and Yamin D 2015 Chapter 7 - Fostering Community Participation Wildfire: Experiences from Indonesia Wildfire Hazards, Risks and Disasters ed J F Shroder and D Paton (Oxford: Elsevier) pp 123–44
- [2] BNPB 2013 Rencana Kontinjensi Nasional Menghadapi Ancaman Bencana Asap Akibat Kebakaran Hutan dan Lahan ed F Irawan (Jakarta)
- [3] Dennis R 1999 A review of fire projects in Indonesia, 1982–98
- [4] Yadav I C, Linthoingambi Devi N, Li J, Syed J H, Zhang G and Watanabe H 2017 Biomass burning in Indo-China peninsula and its impacts on regional air quality and global climate change-a review Environ. Pollut. 227 414–27

- [5] Radojevic M 2003 Chemistry of forest fires and regional haze with emphasis on Southeast Asia *Pure Appl. Geophys.* 160 157–87
- [6] Shrestha G, Traina S J and Swanston C W 2010 Black carbon's properties and role in the environment: A comprehensive review *Sustainability* 2 294–320
- [7] Ramachandran S and Kedia S 2010 Black carbon aerosols over an urban region: Radiative forcing and climate impact *J. Geophys. Res. Atmos.* 115
- [8] Reyna-Bensusan N, Wilson D C, Davy P M, Fuller G W, Fowler G D and Smith S R 2019 Experimental measurements of black carbon emission factors to estimate the global impact of uncontrolled burning of waste *Atmos. Environ.* 213 629–39
- [9] Wargan K, Labow G, Frith S, Pawson S, Livesey N and Partyka G 2017 Evaluation of the ozone fields in NASA's MERRA-2 reanalysis *J. Clim.* 30 2961–88
- [10] Link D, Wang Z and Xiong X 2016 Status of MODIS spatial and spectral characterization and performance *Earth Obs. Mission. Sensors Dev. Implementation, Charact.* IV 9881 98811G
- [11] Sabani W, Rahmadewi D P, Rahmi K I N, Priyatna M and Kurniawan E 2019 Utilization of MODIS data to analyze the forest/land fires frequency and distribution (Case Study : Central Kalimantan Province *IOP Conf. Series: Earth and Environmental* 243 2–3
- [12] Giglio L, Schroeder W, Justice CO 2016 The collection 6 MODIS active fire detection algorithm and fire products. *Remote Sens Environ* 178 31–41
- [13] Urraca R, Huld T, Gracia-Amillo A, Martinez-de-Pison F J, Kaspar F and Sanz-Garcia A 2018 Evaluation of global horizontal irradiance estimates from ERA5 and COSMO-REA6 reanalyses using ground and satellite-based data *Sol. Energy* 164 339–54
- [14] Hersbach H, Bell B, Berrisford P, Hirahara S, Horányi A, Muñoz-Sabater J, Nicolas J, Peubey C, Radu R, Schepers D, Simmons A, Soci C, Abdalla S, Abellan X, Balsamo G, Bechtold P, Biavati G, Bidlot J, Bonavita M, De Chiara G, Dahlgren P, Dee D, Diamantakis M, Dragani R, Flemming J, Forbes R, Fuentes M, Geer A, Haimberger L, Healy S, Hogan R J, Hólm E, Janisková M, Keeley S, Laloyaux P, Lopez P, Lupu C, Radnoti G, de Rosnay P, Rozum I, Vamborg F, Villaume S and Thépaut J-N 2020 The ERA5 global reanalysis *Q. J. R. Meteorol.Soc.* 146 1999–2049
- [15] Akpınar E K, Akpınar S and Öztıp H F 2009 Statistical analysis of meteorological factors and air pollution at winter months in Elazığ, Turkey *J. Urban Environ. Eng.* 3 7–16
- [16] Stein A F, Draxler R R, Rolph G D, Stunder B J B, Cohen M D and Ngan F 2015 NOAA's hysplit atmospheric transport and dispersion modeling system *Bull. Am. Meteorol. Soc.* 96 2059–77
- [17] Rolph G, Stein A and Stunder B 2017 Real-time Environmental Applications and Display sYstem: READY *Environ. Model. Softw.* 95 210–28
- [18] Arisman 2020 Analisis Tren Kebakaran Hutan dan Lahan di Indonesia Periode Tahun 2015-2019 Trend Analysis of Forest and Land Fires in Indonesia periods 2015-2019 *J. Sains Teknol.Lingkung.* 6 1–9
- [19] Rajendran K, Kitoh A and Yukimoto S 2004 South and East Asian summer monsoon climate and variation in the MRI coupled model (MRI-CGCM2) *J. Clim.* 17 763–82
- [20] Hendon H H 2003 Indonesian rainfall variability: Impacts of ENSO and local air-sea interaction *J. Clim.* 16 1775–90
- [21] Heriyanto E and Nuryanto D E 2014 Prediksi Sebaran Asap Kebakaran Hutan/Lahan Menggunakan WRF/CHEM (Studi Kasus: Tanggal 14 dan 20 Juni 2012, Pekanbaru-Riau) *J. Meteorol. dan Geofis.* 15 51–8
- [22] Aldrian E 2011 Adaptasi dan mitigasi perubahan iklim global *Prasetya Online* 174
- [23] Hayasaka H, Usup A and Naito D 2020 New approach evaluating peatland fires in Indonesian factors *Remote Sens.* 12
- [24] Stiegler C, Meijide A, Fan Y, Ashween Ali A, June T and Knohl A 2019 El Niño-Southern Oscillation (ENSO) event reduces CO₂ uptake of an Indonesian oil palm plantation *Biogeosciences* 16 2873–90
- [25] Qian J H, Robertson A W and Moron V 2013 Diurnal cycle in different weather regimes and rainfall variability over borneo associated with ENSO *J. Clim.* 26 1772–90
- [26] Sitnov S A, Mokhov I I and Likhoshesterova A A 2020 Exploring large-scale black-carbon air pollution over Northern Eurasia in summer 2016 using MERRA-2 reanalysis data *Atmos. Res.* 235 104763
- [27] KLHK 2019 Analisa Data Luas Areal Kebakaran Hutan & Lahan
- [28] Cape J N, Coyle M and Dumitrescu P 2012 The atmospheric lifetime of black carbon *Atmos. Environ.* 59 256–63
- [29] Chen W and Guan Z 2017 A joint monsoon index for East Asian–Australian monsoons during boreal summer *Atmos. Sci. Lett.* 18 403–408